Check for updates

# Establishment and validation of a novel anoikis-related prognostic signature of clear cell renal cell carcinoma

Yankuo Liu[1†], Zhiyuan Shi[1†], Jianzhong Zheng[1†], Zeyuan Zheng[1], Huimin Sun[2], Zuodong Xuan[1], Yang Bai[1], Meiling Fu[1], Yifan Du[1] and Chen Shao[1*]

[1]Department of Urology, Xiang'an Hospital of Xiamen University, School of Medicine, Xiamen University, Xiamen, China, [2]Central Laboratory, Xiang'an Hospital of Xiamen University, School of Medicine, Xiamen University, Xiamen, China

**Background:** Despite progression in its treatment, the clinical outcome of patients with clear cell renal cell carcinoma (ccRCC) remains not ideal. Anoikis is a unique form of programmed apoptosis, owing to insufficient cell-matrix interactions. Anoikis plays a crucial role in tumor migration and invasion, and tumor cells could protect themselves through the capacity of anoikis resistance.

**Methods:** Anoikis-related genes (ARGs) were obtained from Genecards and Harmonizome portals. The ARGs related to ccRCC prognosis were identified through univariate Cox regression analysis, then we utilized these ARGs to construct a novel prognostic model for ccRCC patients. Moreover, we explored the expression profile of ARGs in ccRCC using the Cancer Genome Atlas (TCGA) and Genotype-Tissue Expression (GTEx) database. We also conducted Real-Time Polymerase Chain Reaction (RT-PCR) to probe ARGs expression of the risk score. Finally, we performed correlation analysis between ARGs and tumor immune microenvironment.

**Results:** We identified 17 ARGs associated with ccRCC survival, from which 7 genes were chosen to construct a prognostic model. The prognostic model was verified as an independent prognostic indicator. The expression of most ARGs was higher in ccRCC samples. These ARGs were closely correlated with immune cell infiltration and immune checkpoint members, and had independent prognostic value respectively. Functional enrichment analysis demonstrated that these ARGs were significantly associated with multiple types of malignances.

**Conclusion:** The prognostic signature was identified to be highly efficient in predicting ccRCC prognosis, and these ARGs were closely related to tumor microenvironment.

KEYWORDS

anoikis, clear cell renal cell carcinoma, prognostic model, tumor microenvironment, bioinformatics

## Introduction

Renal cell carcinoma (RCC) is one of the predominant tumors in urological system, and there is an increasing number of new patients with RCC year by year (1, 2). Clear cell RCC (ccRCC) is the most frequent pathological subtype of RCC, with a ratio of 75-80% (3). The clinical prognosis of RCC patients is closely associated with disease pathological stage, and relapse-free survival rate is decreasing from stage I to stage IV (4). Early surgical resection is considered as the predominant treatment for ccRCC patients (5). However, about 40% of patients with surgical treatment occur distant metastases, contributing to poor endpoint (4). For patients with metastatic or unresectable RCC, targeted therapy drugs were demonstrated to prolong survival time effectively, including sorafenib and sunitinib (6, 7). However, various of adverse effects decrease the life quality of patients during target treatment, such as hypertension (8). Thus, there is an urgent need to perform early diagnosis of ccRCC, finding novel diagnosis biomarkers and prognostic signatures have great clinical benefit.

Epithelial cells in human body keep normal tissue structure by cell-to-cell adherence and cell-to-extracellular matrix interactions (9). Four cell adhesion protein molecules are involved in these interactions, including: cadherins, immunoglobulins, selectins, and integrins. Anoikis is a kind of specific programmed apoptosis which occurs when cell-to-cell adherence and cell-to-extracellular matrix interactions are destroyed, and it plays an important role in maintaining tissue homeostasis by killing misplaced cells (10). Mitochondria- and cell surface death receptor-mediated pathways are necessary for triggering anoikis (11). In diverse tumors, anoikis serves as a protective physiological barrier inhibiting dissemination of metastatic cancer cells. However, cancer cells have the power of anoikis resistance to guarantee their survival *via* different signaling pathways, resulting in the distant metastasis (12). Previous studies have demonstrated that anoikis-related genes (ARGs) were closely correlated with metastatic cascade and progression of cancer. As a member of ARGs, the expression of Fas apoptotic inhibitory molecule 2 (FAIM2) was positively linked to tumor stage and poor endpoint of non-small cell lung cancer, and FAIM2 knockdown may inhibit anoikis resistance (13). Kruppel-like factor 5 (KLF5) was verified to promote anoikis resistance, and elevated KLF5 expression was correlated with poor clinical outcome in colorectal cancer patients (14).

Past studies have validated that several ARGs were involved in reversing anoikis resistance and invasion and migration in RCC (15, 16). Nevertheless, few studies have systematically explored the role of ARGs in ccRCC. In our study, multiple databases are integrated to screen seven ARGs. Then, the anoikis prognostic model (APM) based on these seven ARGs was constructed and validated. Finally, we performed several analyses to explore the expression profile of these ARGs and the correlation between immune cell infiltration and ARGs expression in ccRCC.

## Materials and methods

### Data collection and processing

We downloaded the GSE53757 (72 normal renal samples and 72 ccRCC samples), GSE40435 (101 normal renal samples and 101 ccRCC samples), and GSE66272 (27 normal renal samples and 27 ccRCC samples) datasets from the GEO database (https://www.ncbi.nlm.nih.gov/geo/, accessed on 12 October 2022). Then we obtained 316 anoikis-related genes from the genecards website (17) (https://www.genecards.org/, accessed on 12 October 2022) and Harmonizome portals (18) (https://maayanlab.cloud/Harmonizome/, accessed on 12 October 2022). The above data analysis was performed by R software. The ARGs expression data was normalized *via* the "edgeR" package (19). We obtained the differentially expressed genes (DEGs) between ccRCC tissues and normal kidney samples in the GSE53757, GSE40435, GSE66272, and KIRC datasets by "limma" package. Furthermore, we collected the tumor prognostic genes (TPGs) *via* "survival" package, and overall survival (OS) of these genes was verified using univariate Cox analysis (20).

### Construction and validation of the APM

We utilized the least absolute shrinkage and selection operator (LASSO) Cox regression analysis to screen out ARGs which were closely associated with prognosis of ccRCC patients, and optimal lambda ($\lambda$) was seen as the optimal value *via* cross validation (21, 22). Then we computed the risk score by integrating the expression profile of ARGs and paired multivariate Cox regression values ($\beta$). We divided the ccRCC patients into two groups (low-risk group and high-risk group) based on the media risk score. The "umap" package and "Rtsne" package were used to demonstrate the distribution patterns of ccRCC patients. We utilized the "survminer" package to perform Kaplan-Meier (K-M) survival analysis. The "time" ROC package was used to perform time-dependent receiver operating characteristic (ROC) analysis.

### Predictive role of the APM

A heatmap was employed to demonstrate the APM and clinical characteristics including age, grade, gender, and stage of patients. We used the univariate and multivariate Cox regression analyses to evaluate the predictive value of the APM and several clinical factors.

### Construction and validation of the nomogram

The "survival" package and "rms" package were employed to build a nomogram predicting prognosis based on the Cox regression analysis results. We used the calibration curve to estimate the predictive effectiveness of the nomogram. The "time" ROC package was utilized to perform the time-dependent ROC analysis which could estimate the precision of the APM.

### Gene expression analysis of ARGs

In our study, we utilized R (version3.6.3) to analyze the mRNA expression levels of the ARGs in tumor tissues and paracancerous

tissue samples in The Cancer Genome Atlas (TCGA) and normal kidney tissues in Genotype-Tissue Expression (GTEx) database which were downloaded from UCSC Xena website (https://xena.ucsc.edu/) (23). The expression profile was visualized with ggplot2 (3.3.3). Then we evaluated the statistical significance of the differential expression by using the Wilcoxon test. The total protein expression levels of ARGs were collected from Clinical Proteomic Tumor Analysis Consortium (CPTAC) dataset in the UALCAN website (http://ualcan.path.uab.edu/analysis-prot.html), a convenient tool for exploring cancer omics data (24).

## Immune infiltration analysis

R package "estimate" was employed to investigate the abundance of stromal components (StromalScore), immune cell infiltration levels (ImmuneScore) and ESTIMATEScore of ccRCC. The associations between ARGs expression and immune/stromal/estimate scores were evaluated by Spearman's correlation analysis. The CIBERSORT algorithm was utilized to conduct the immune cell infiltration estimations (25). The partial correlation (cor) values and $p$ values were calculated *via* the purity-adjusted Spearman's rank correlation test.

## Functional and pathway enrichment analysis

With the help of GeneMANIA website (http://www.genemania.org), we explored and displayed the interaction network among these seven ARGs. We used WebGestalt to perform Gene Ontology (GO) and Kyoto Encyclopedia of Genes and Genomes (KEGG) analysis about ARGs in ccRCC.

## Cell culture

We obtained three human ccRCC cell lines 786-O, Caki-1 and ACHN and human renal proximal convoluted tubule cell HK2 from American Type Cultural Collection (ATCC). 786-O and Caki-1 were cultured in RPMI 1640 media (11875119, Gibco, Foster, CA, USA). HK2 and ACHN were kept in DMEM high glucose media (11965092, Gibco, Foster, CA, USA). All media contained 1% penicillin-streptomycin (15140163, Gibco, Foster, CA, USA) solution and 10% fetal bovine serum (FBS) (10100147, Gibco, Foster, CA, USA). All cells were maintained in an incubator at 37°C with a 5% $CO_2$.

## Reverse transcription and PCR analysis

Total RNA from cells was extracted by using the Spark easy cellular RNA extraction kit (AC0205) (Shandong Sparkjade Biotechnology Co., Ltd). The Evo M-MLV RT Kit (AG11711) was obtained from Accurate Biotechnology (Hunan) Co., Ltd. The

Hieff®qPCR SYBR Green Master Mix (11201ES08) were obtained from Yeasen Biotechnology (Shanghai) Co., Ltd. (Shanghai, China). The primer sequences of RT-qPCR were displayed in Table S1.

## Statistical analysis

All data were demonstrated by mean ± standard deviation. Statistical analysis was conducted by using SPSS 13. The value of $p < 0.05$ was considered significant (* $p < 0.05$, ** $p < 0.01$, *** $p < 0.001$, **** $p < 0.0001$). The "ns" represented no statistically significant.

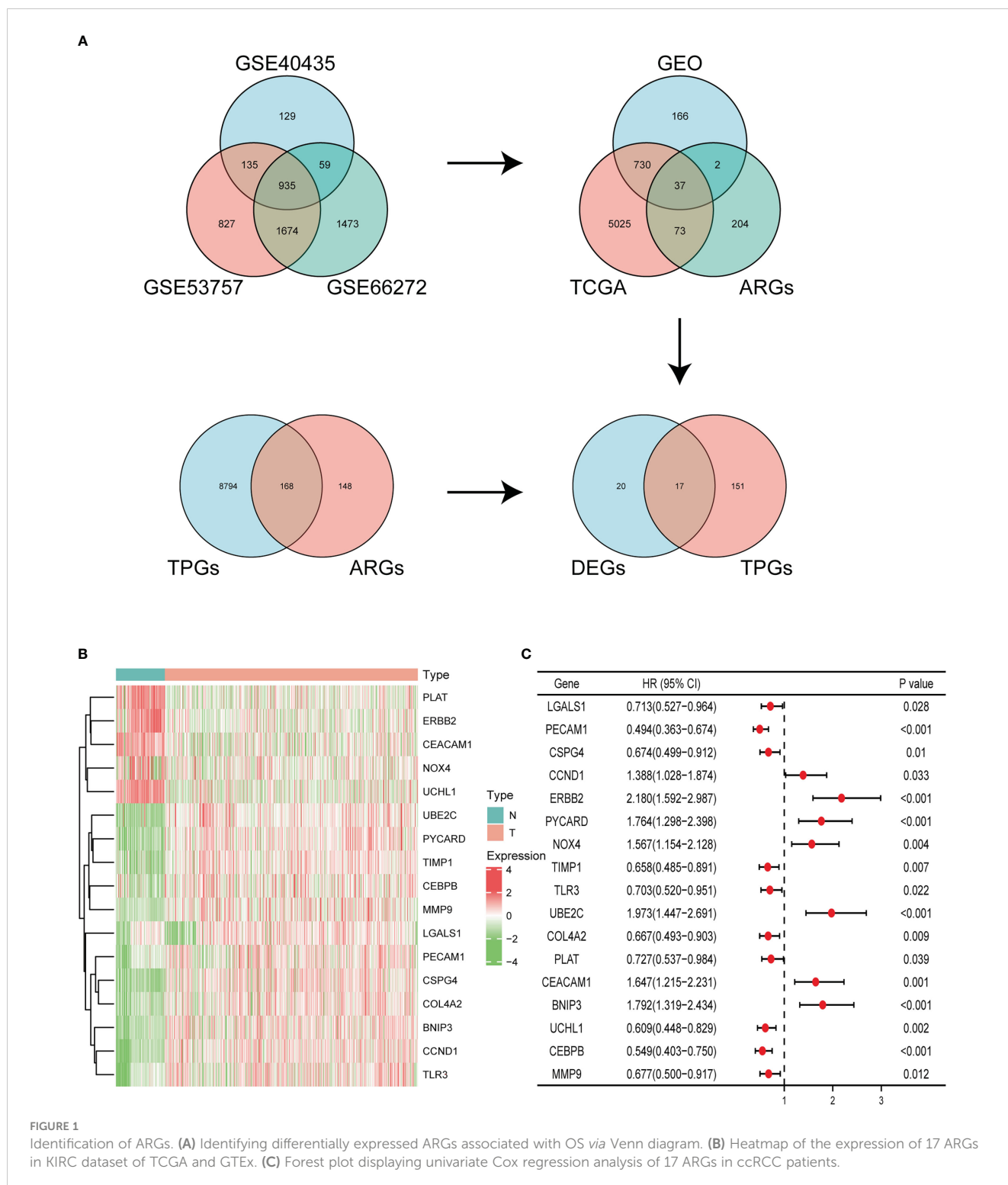# Results

## Identification of the ARGs

In our study, a total of 935 DEGs were identified from three GEO databases, including GSE40435, GSE53757, and GSE66272. Then we obtained 37 significant DEGs from GEO dataset, TCGA database, and ARGs. In addition, we identified 168 TPGs based on ARGs and TPGs database. Finally, we integrated the 37 significant DEGs and 168 TPGs and screened out 17 genes (Figure 1A). In these genes, 12 genes expression were upregulated in ccRCC tissues compared with normal kidney samples in TCGA and GTEx, including UBE2C, PYCARD, TIMP1, CEBPB, MMP9, LGALS1, PECAM1, CSPG4, COL4A2, BNIP3, CCND1, TLR3. While 5 genes were downregulated in tumor tissues, including PLAT, ERBB2, CEACAM1, NOX4, and UCHL1 (Figure 1B). Univariate Cox regression analysis demonstrated that 17 ARGs were closely linked to clinical outcome of ccRCC patients (Figure 1C).
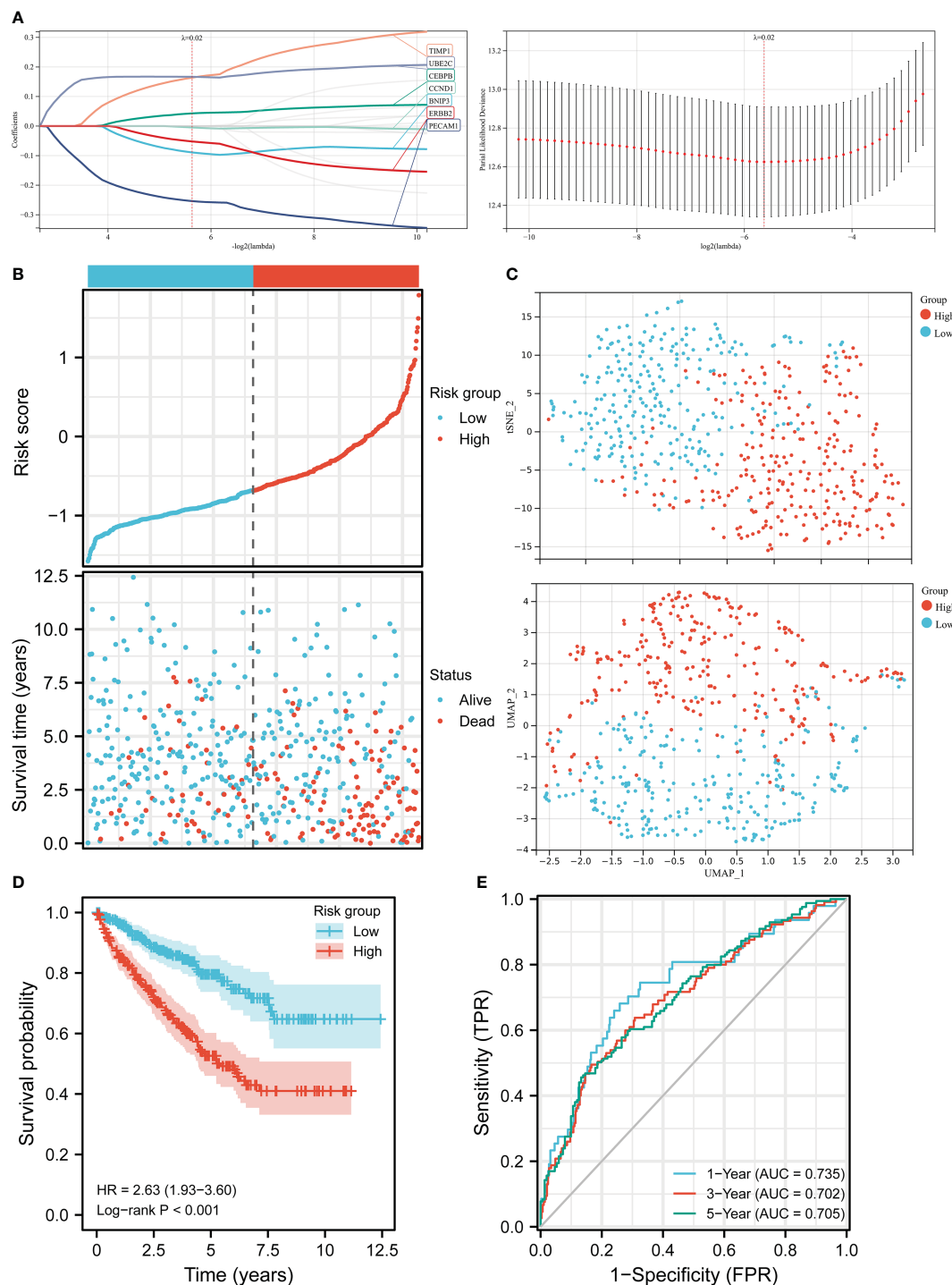
## Construction of the APM

LASSO regression analysis was employed to identify seven prognosis-related genes including BNIP3, CCND1, CEBPB, ERBB2, PECAM1, TIMP1, and UBE2C from 17 ARGs (Figure 2A). By weighting the expression of these seven genes with LASSO regression coefficient, we constructed the APM based on the following algorithm. Risk score = (-0.08912 * BNIP3 expression) + (-0.00457 * CCND1 expression) + (0.04290 * CEBPB expression) + (-0.05204 * ERBB2 expression) + (-0.25383 * PECAM1 expression) + (0.16386 * TIMP1 expression) + (0.16675 * UBE2C expression). We firstly checked the clinical information and gene expression profiles of the ccRCC patients in TCGA, 13 cases without gene expression and unabridged clinical data were deleted. Then 526 patients were grouped into a high-risk cluster (n = 263) and a low-risk cluster (n = 263) according to the media risk score. The survival time of patients in high-risk group was shorter than patients in low-risk group (Figure 2B). The UMAP and t-SNE analysis demonstrated that the distribution of ccRCC patients in two groups was in line with the expectation (Figure 2C). The K-M

**FIGURE 1**

Identification of ARGs. **(A)** Identifying differentially expressed ARGs associated with OS *via* Venn diagram. **(B)** Heatmap of the expression of 17 ARGs in KIRC dataset of TCGA and GTEx. **(C)** Forest plot displaying univariate Cox regression analysis of 17 ARGs in ccRCC patients.

curve indicated that the OS of high-risk group was lower than that of low-risk group (Figure 2D). ROC analysis was employed to evaluate the predictive performance of the APM, and the area under curve (AUC) values in 1-year, 3-year, 5-year were 0.735, 0.702, and 0.705, respectively, suggesting that the APM could be an ideal prognosis indicator (Figure 2E).

## Independent prognostic value of the APM and construction of the nomogram

The heatmap demonstrated the correlation between risk group, stage, grade, gender, age, status, and expression levels of seven ARGs (Figure 3A). A higher risk score was found to be associated

FIGURE 2

Construction of the risk score model in TCGA. **(A)** LASSO regression analysis and LASSO coefficient profiles of ARGs. **(B)** Risk score distribution and ccRCC patients' survival status. **(C)** UMAP plot and t-SNE plot of the ccRCC patients exhibiting the distribution in high and low-risk groups. **(D)** K-M curves of patients in high and low-risk groups. **(E)** AUC of the time-dependent ROC curves.

with higher expression levels of UBE2C, CEBPB, TIMP1, and lower expression levels of ERBB2, BNIP3, CCND1, PECAM1. A univariate Cox regression analysis indicated that age, cancer grade, risk score and tumor stage were closely correlated with OS (Figure 3B). Meanwhile, a multivariate Cox regression analysis displayed that risk score, age, and tumor stage were significantly

related to OS (Figure 3C). These results indicated that the APM had independent prognostic value in ccRCC patients. Next, we constructed a nomogram about age, stage, and risk score to compute the survival probability rates (Figure 3D). The 1-, 3-, and 5-year AUCs for the nomogram were 0.867, 0.810, and 0.777, respectively (Figure 3E). Furthermore, the calibration plot also
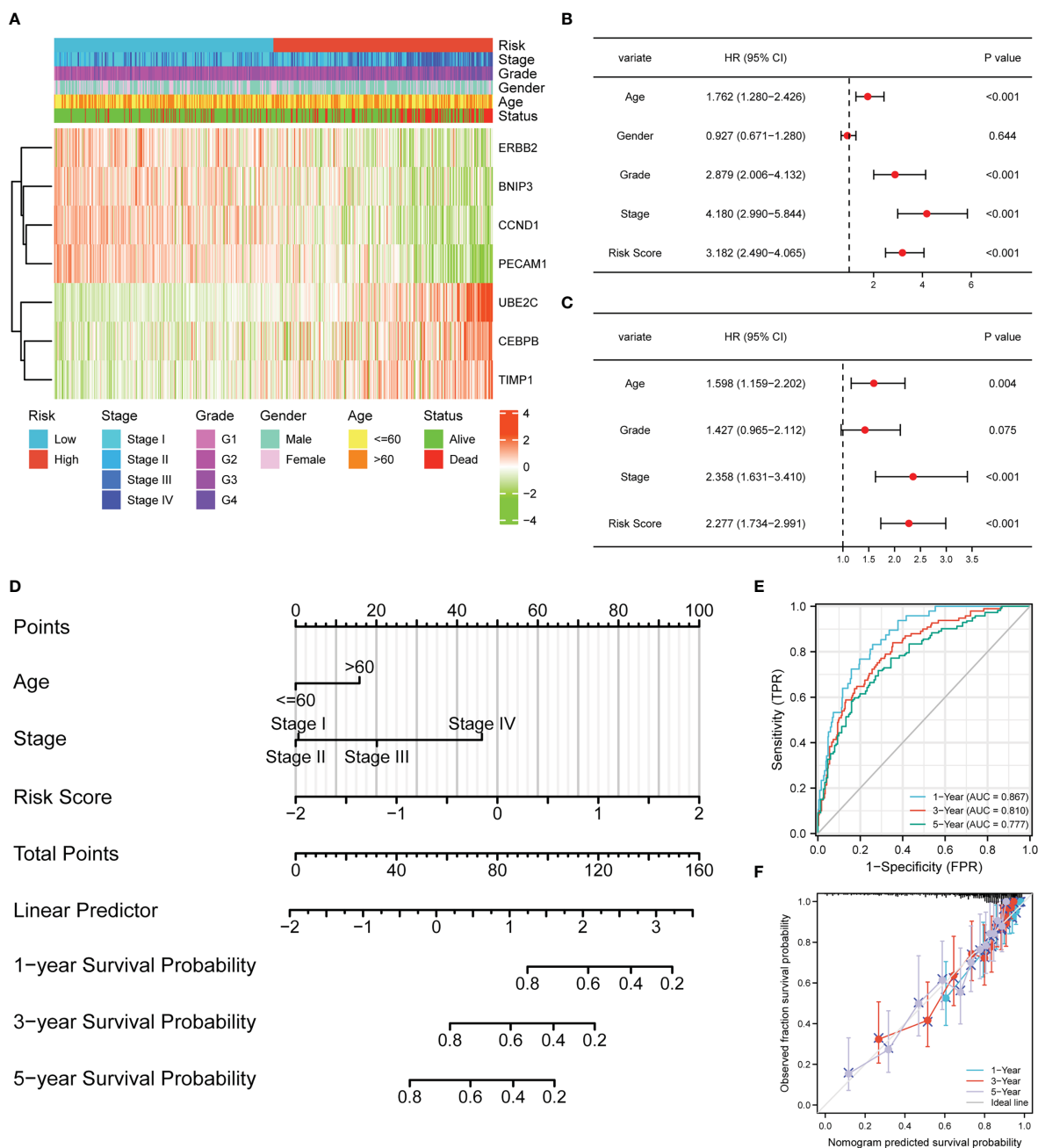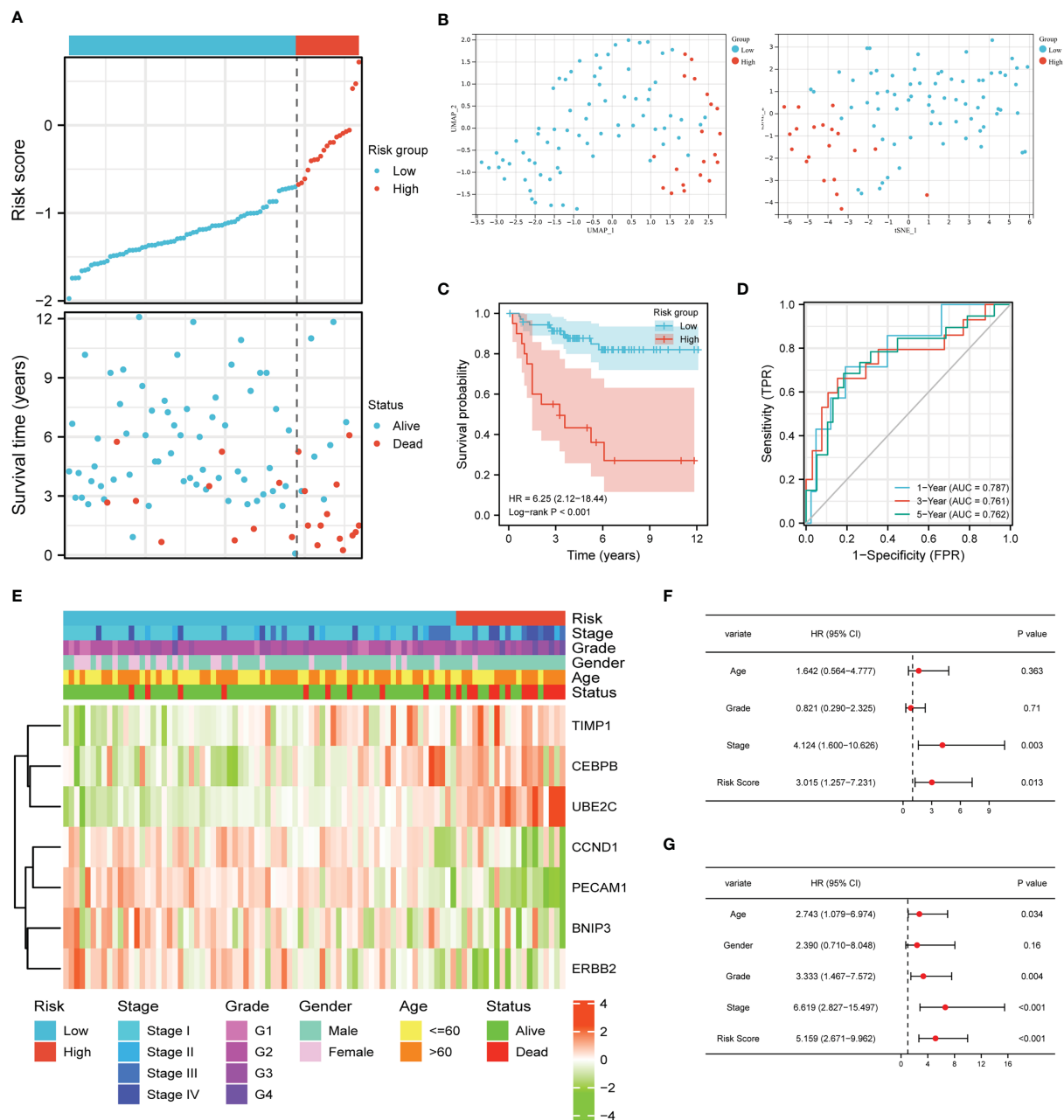
**FIGURE 3**

The risk score model could be an independent prognostic indicator for ccRCC. **(A)** Heatmap demonstrating the association between ARGs expression and clinical factors and risk groups. **(B)** Univariate Cox regression analysis of ccRCC patients in TCGA. **(C)** Multivariate Cox regression analysis of ccRCC patients in TCGA. **(D)** Nomogram-based gene signature for predicting 1-, 3- and 5-year OS. ROC curves **(E)** and calibration curves **(F)** for predicting the 1-, 3-, and 5-year performance of the nomogram.

demonstrated the ideal prediction effect at 1-, 3-, and 5-year OS (Figure 3F).

## Validation of the APM in E-MTAB-1980 cohort

The clinical feature and gene expression profile of the patients in E-MATB-1980 cohort were checked, and patients with abridged

information were deleted from the cohort. Then we chose 92 cases to verify the prognostic value of the APM, which were divided into a low-risk group (n = 33) and a high-risk group (n = 59) based on the media risk score. Figure 4A demonstrated that most dead patients were distributed into the high-risk group, suggesting the ideal predictive value of the risk score. UMAP and t-SNE analysis displayed that the ccRCC patients of two groups could be placed into two sets suitably (Figure 4B). The K-M curve indicated that the high-risk group patients had a worse clinical outcome, and the AUC

**FIGURE 4**

Validation of the risk score model. **(A)** Risk score distribution and ccRCC patients' survival status. **(B)** UMAP plot and t-SNE plot of the ccRCC patients exhibiting the distribution in high and low-risk groups. **(C)** K-M curves of patients in high and low-risk groups. **(D)** AUC of the time-dependent ROC curves. **(E)** Heatmap demonstrating the association between ARGs expression and clinical factors and risk groups. Univariate Cox regression analysis **(F)** and multivariate Cox regression analysis **(G)** of ccRCC patients.

values in 1-year, 3-year, 5-year were 0.787, 0.761, and 0.762, respectively (Figures 4C, D). The heatmap demonstrated the correlation between expression levels of these seven ARGs and risk group, clinical information, and pathological characteristic (Figure 4E). The univariate Cox regression analysis showed that stage and risk score were closely related to OS (Figure 4F). Meanwhile, the age, grade, stage, and risk score had an intimate relationship with OS in multivariate Cox regression (Figure 4G).

These results further verified the independent prognostic value of the APM.

## Expression profiles of ARGs in ccRCC

Next, we explored the expression patterns of these seven ARGs in ccRCC tissues and paired normal kidney samples based on

TCGA dataset. As graphed in Figure 5A, the mRNA expression levels of BNIP3, CCND1, CEBPB, PECAM1, TIMP1, and UBE2C were higher than that in normal kidney tissues, while ERBB2 was downregulated in ccRCC. The protein expression levels of BNIP3, CCND1, PECAM1, TIMP1, and UBE2C were elevated in ccRCC, while CEBPB and ERBB2 protein expression were downregulated in ccRCC (Figure 5B).

Furthermore, we chose human ccRCC cell lines 786-O, Caki-1 and ACHN and human renal proximal convoluted tubule cell HK2 to detect the expression of ARGs *via* RT-qPCR experiments. As
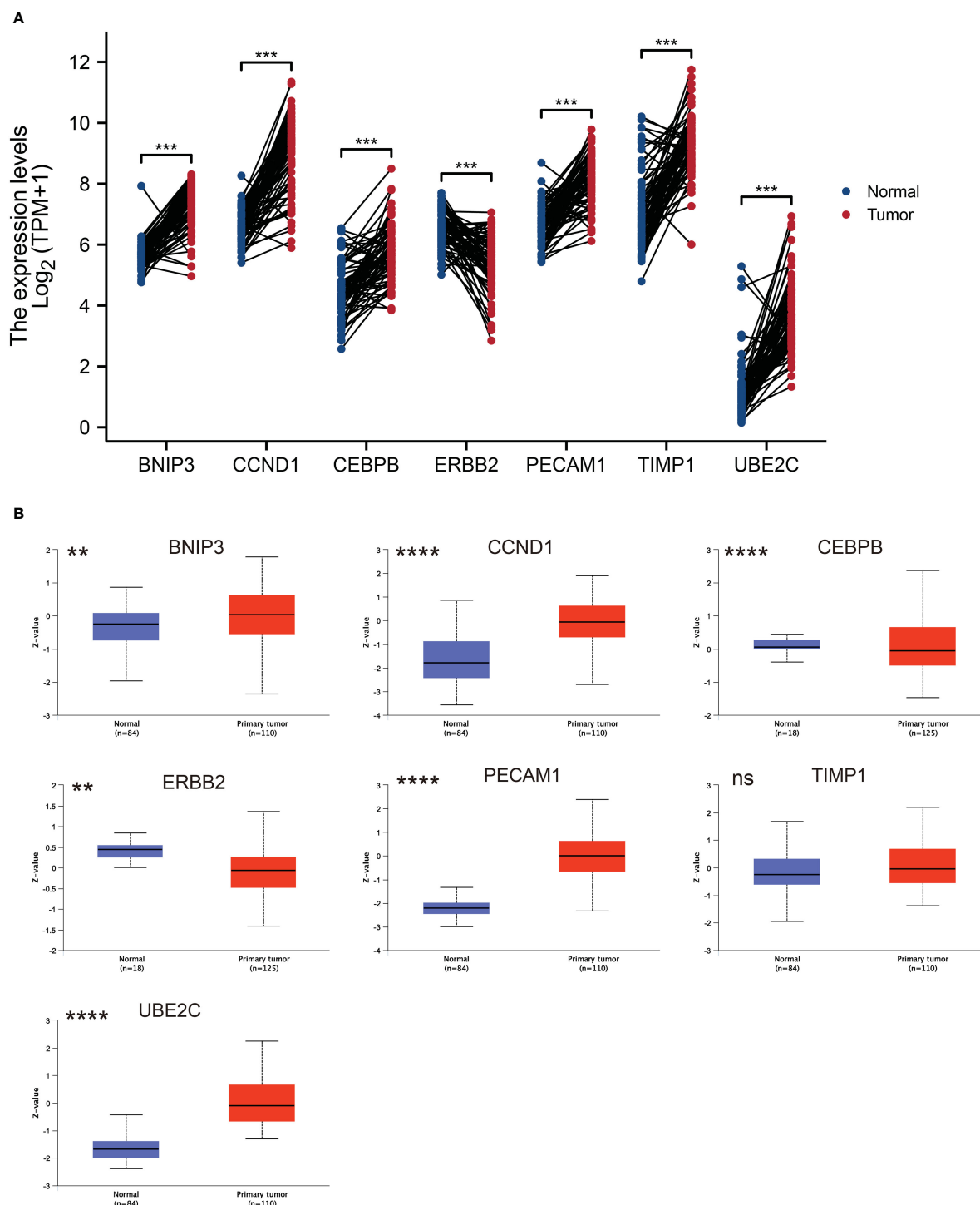


**FIGURE 5**

ARGs expression profiles in ccRCC and normal tissues. **(A)** Expression levels of ARGs in ccRCC and paired normal tissue samples. The red color represents tumor tissue, while the blue color represents normal tissue. **(B)** Total protein levels of ARGs in ccRCC and normal tissue samples from CPTAC. ** $p < 0.01$, *** $p < 0.001$, **** $p < 0.0001$. ns represents no significance.

displayed in Figure 6, the mRNA expression levels of CCND1 and CEBPB were higher in three ccRCC cell lines than that in HK2, and BNIP3 and PECAM1 were higher expressed in 786-O and Caki-1 than HK2. We also conducted immunohistochemistry (IHC) staining to investigate the UBE2C protein level in ccRCC and par-carcinoma tissue. The result demonstrated that UBE2C protein level was significantly upregulated in ccRCC compared to par-carcinoma tissue, which was consistent with previous result from CPTAC (Figure S1).

## Clinicopathological stages and independent prognostic value of ARGs in ccRCC

As displayed in Figure S2, the expression levels of these seven ARGs were strongly correlated with pathological stages of ccRCC patients. Notably, the expression levels BNIP3, CCND1, ERBB2, and PECAM1 were downregulated from stage I to stage IV in ccRCC, while expression of CEBPB, TIMP1, and
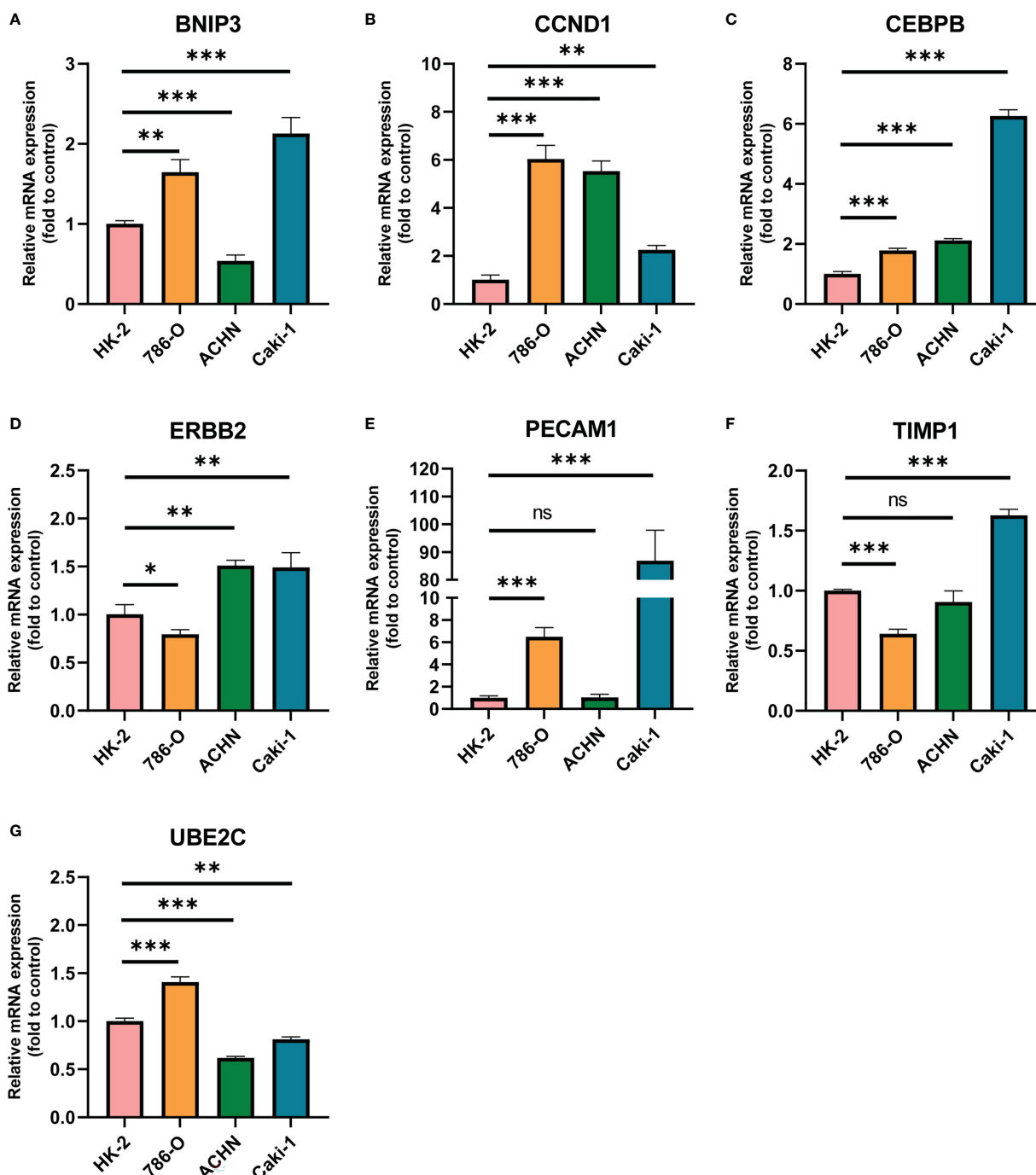


FIGURE 6

The mRNA expression of ARGs in HK2 and three ccRCC cell lines quantified by real-time PCR. **(A)** BNIP3; **(B)** CCND1; **(C)** CEBPB; **(D)** ERBB2; **(E)** PECAM1; **(F)** TIMP1; **(G)** UBE2C. * $p < 0.05$, ** $p < 0.01$, *** $p < 0.001$, **** $p < 0.0001$. ns represents no significance.

UBE2C were elevated in higher stage. To further explore the independent prognostic value of single ARGs in ccRCC, we performed survival analysis using K-M plotter. The result demonstrated that high expression levels of BNIP3, CCND1, ERBB2, and PECAM1 were correlated with better clinical endpoint of ccRCC, while high CEBPB, TIMP1, and UBE2C expression were linked to worse clinical outcome (Figure S3). The K-M result was consistent with previous Cox regression analysis.

## TME and immune infiltration analysis of ARGs

An increasing number of evidences have illustrated that tumor microenvironment (TME) plays a significant role in tumor occurrence and progression (26, 27). Therefore, it is essential to dig out the relationship between expression of ARGs and TME. In our study, the ESTIMATE algorithm was utilized to evaluate the immune and stromal scores of ccRCC. Figure 7 demonstrated that
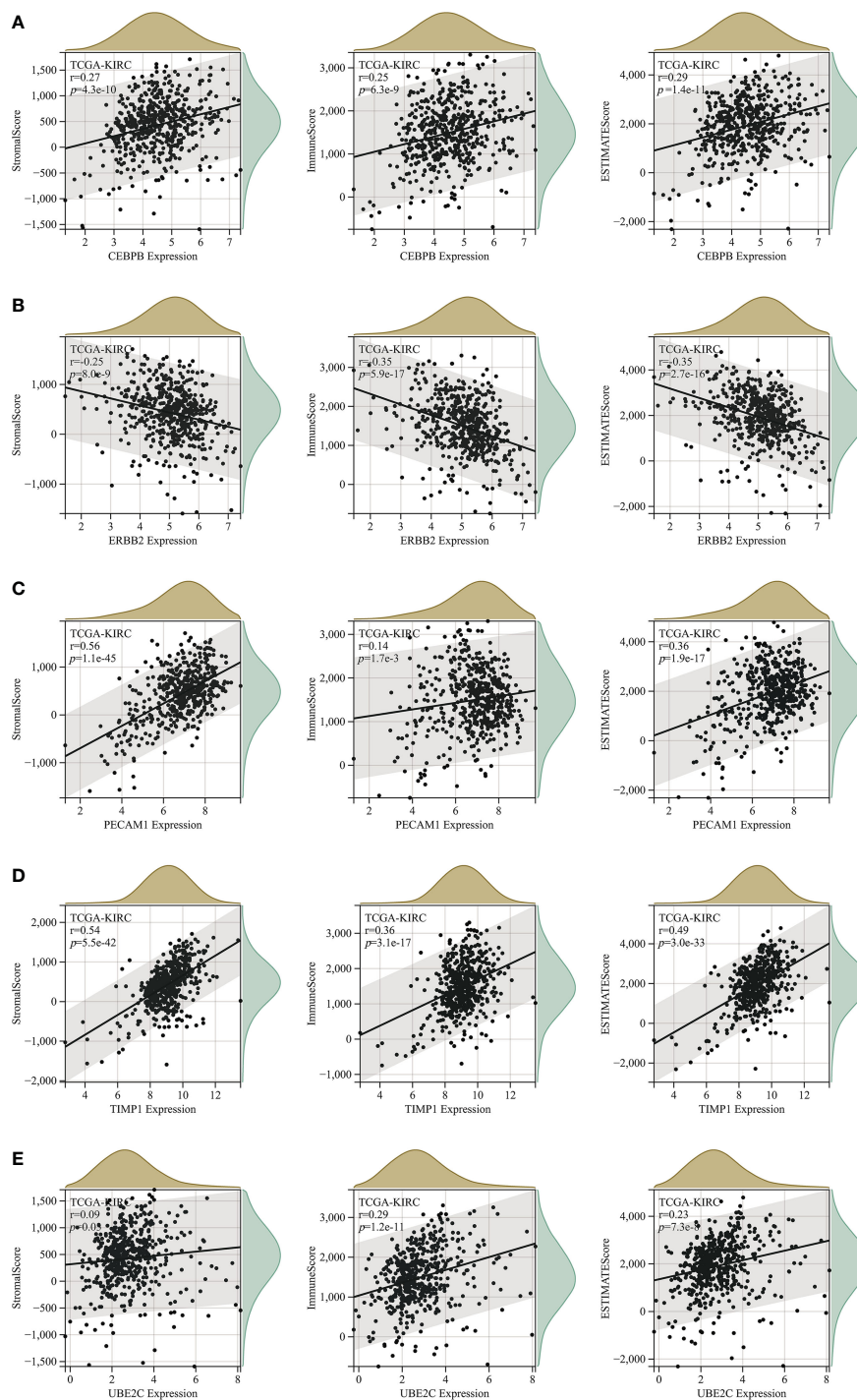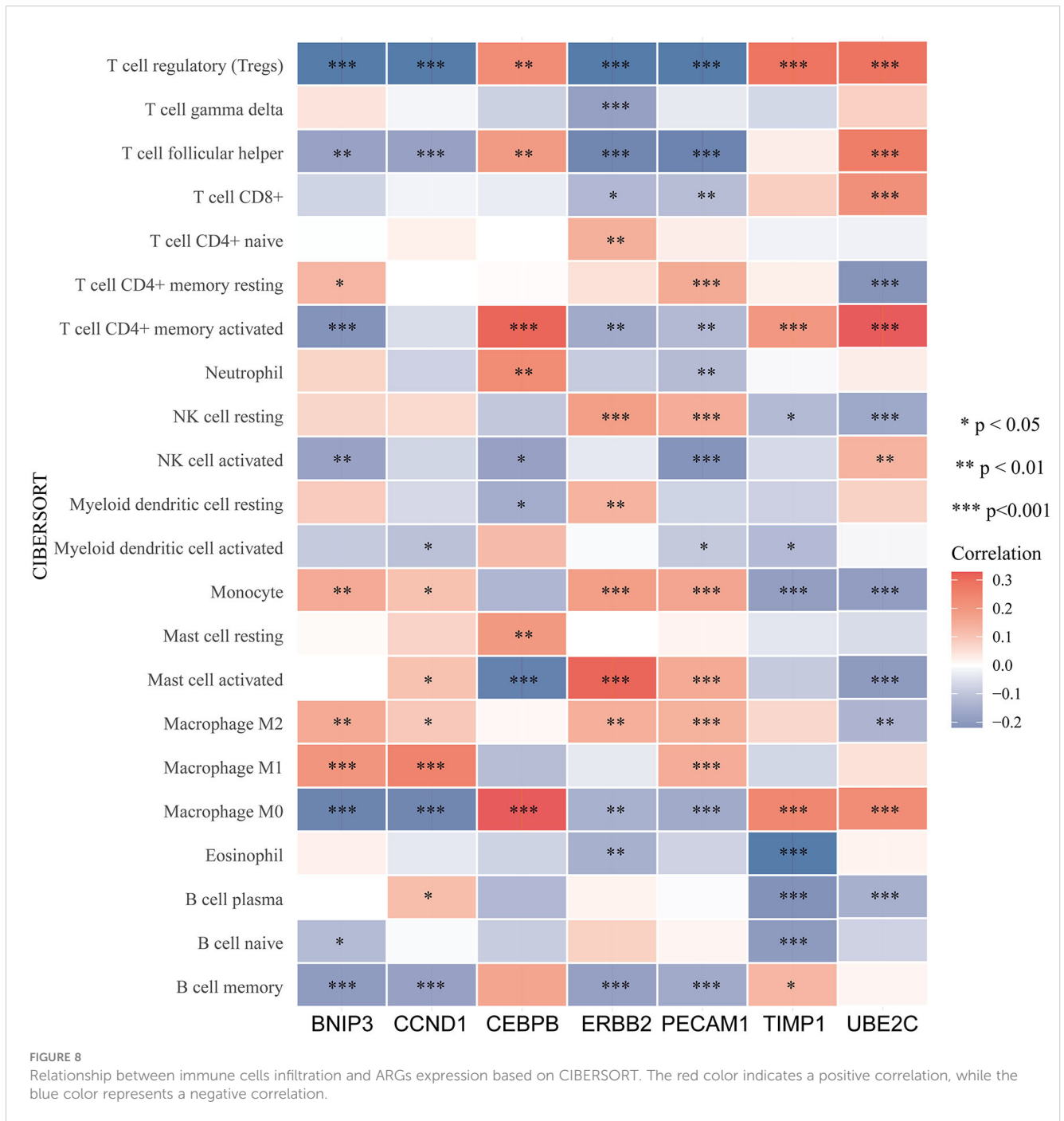


**FIGURE 7**
The correlation analysis between StromalScore, ImmuneScore and ESTIMATEScore and expression levels of **(A)** CEBPB; **(B)** ERBB2; **(C)** PECAM1; **(D)** TIMP1; **(E)** UBE2C.

the expression of CEBPB, PECAM1, TIMP1, and UBE2C were significantly positively associated with stromal score, as well as with immune score, while ERBB2 expression was negatively correlated with these scores. The relationship between BNIP3 and CCND1 had no statistical significance (Figure S4). Moreover, we examined the association between expression of ARGs and immune cell infiltration level in ccRCC using CIBERSORT algorithm. As displayed in Figure 7, the expression of BNIP3, CCND1, ERBB2, and PECAM1 were closely negatively related to infiltration levels of regulatory T cell, follicular helper T cell, M0 macrophage, and

memory B cell, and were positively correlated with M2 macrophage and monocyte. CEBPB, TIMP1, and UBE2C expression levels were strongly positively associated with infiltration levels of regulatory T cell, CD4+ memory activated T cell, and M0 macrophage (Figure 8).

In addition, we evaluated the relationship between expression of ARGs and immune subtype in ccRCC, and the result displayed high heterogeneity. Immune subtype consisted of six types, including C1 (wound healing), C2 (IFN-gamma dominant), C3 (inflammatory), C4 (lymphocyte depleted), C5 (immunologically quiet), C6 (TGF-β dominant) (25). BNIP3 and UBE2C were highest expressed in C1,



FIGURE 8

Relationship between immune cells infiltration and ARGs expression based on CIBERSORT. The red color indicates a positive correlation, while the blue color represents a negative correlation.

CCND1 and PECAM1 were highest expressed in C3, CEBPB and TIMP1 were highest in C6, and ERBB2 was highest expressed in C5 (Figure 9A). We also evaluated the relationship between ARGs and significant immune checkpoint genes including CD274 (PD-L1), CTLA4, PDCD1LG2 (PD-L2), LAG3 and PDCD1 (PD-1) in ccRCC. As displayed in Figure 9B, the expression levels of CEBPB, TIMP1 and UBE2C were positively correlated with most immune checkpoint genes except for CD274, indicating that they could be potential targets for immunotherapy.

## Correlation and enrichment analysis of ARGs

The correlation analysis of ARGs was conducted in ccRCC, and result was displayed in Figure 10A. GeneMANIA is an online site which have abundant genetic information and can analyze the correlation among several genes (28). Then, the GeneMANIA websi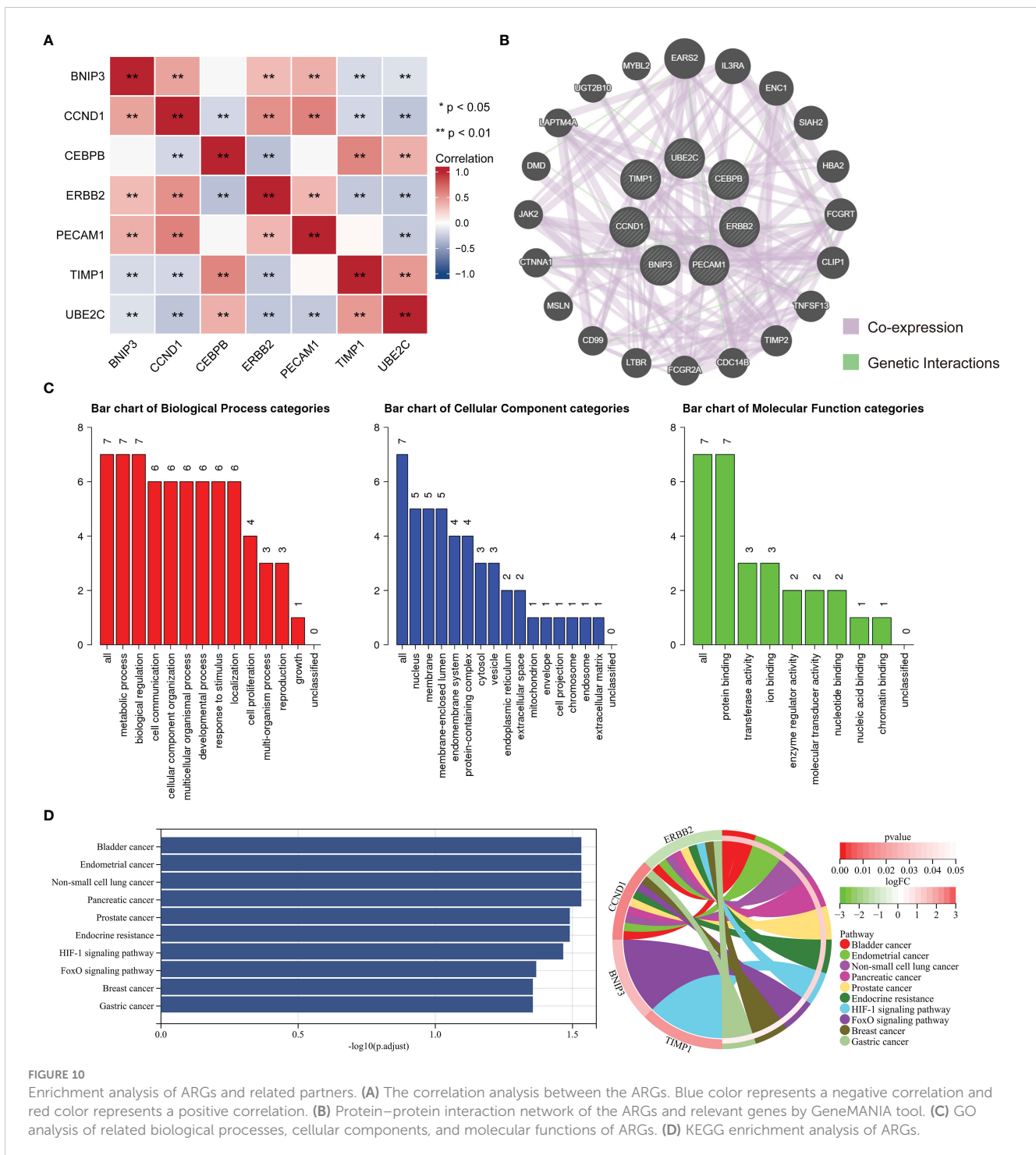te was utilized to explore the several potential interaction partners of ARGs. As showed in Figure 10B, the expression of ARGs



**FIGURE 9**
Correlation analysis between ARGs expression levels and immune subtypes and immune checkpoints in ccRCC. **(A)** ARGs expression in different immune subtypes in ccRCC. C1, wound healing; C2, IFN-g dominant; C3, inflammatory; C4, lymphocyte depleted; C5, immunologically quiet; C6, TGF-β dominant. **(B)** Relationship between ARGs expression and main immune checkpoint genes. The red color indicates a positive association, while the blue color represents a negative association.

FIGURE 10
Enrichment analysis of ARGs and related partners. **(A)** The correlation analysis between the ARGs. Blue color represents a negative correlation and red color represents a positive correlation. **(B)** Protein–protein interaction network of the ARGs and relevant genes by GeneMANIA tool. **(C)** GO analysis of related biological processes, cellular components, and molecular functions of ARGs. **(D)** KEGG enrichment analysis of ARGs.

were closely correlated with EARS2, IL3RA, ENC1 and so on. We next employed GO and KEGG analysis to investigate the biological process, cellular component, molecular function and related signaling pathways of seven ARGs. GO analysis indicated that biological regulation and metabolic process were included in biological process, and protein binding was involved in molecular

function (Figure 10C). The result of KEGG analysis demonstrated that ARGs were involved in occurrence and development of multiple types of tumors, endocrine resistance, and HIF-1 signaling pathway (Figure 10D).

Then, the single cell dataset KIRC_GSE121636 in the TISCH database was employed to explore the expression of ARGs in TME.

In the GSE121636 dataset, CEBPB, PECAM1 and TIMP1 were mainly expressed in monocyte, while ERBB2 was almost not detected in immune cell (Figure S5).

## Discussion

ccRCC was considered as the most common pathological subtype of urologic malignances (29). Several approaches of treating RCC have been employed in clinical work including surgery, radiofrequency ablation, immunotherapy, chemotherapy, and targeted therapy. After radical or partial nephrectomy, plenty of ccRCC patients still develop distant metastases, contributing to higher mortality (30). No enough prognostic indicator or signature has been verified for the clinical outcome of ccRCC patients. Although doctors have made a remarkable progress in treating ccRCC, the endpoint of advanced and metastatic patients is still not ideal (31). The 3-year survival rate of patients with lymph node metastasis is 20-30% after surgery. Targeted therapy including sunitinib has been utilized to treat advanced RCC patients, while large number of patients could acquire drug resistance within 6-15 months, and the OS remains unsatisfactory (32–34). Therefore, it is necessary to explore novel biomarker as the prognostic indicator or therapy target of ccRCC.

Anoikis is a significant defense mechanism, restraining the readhesion of shedding cells to an inappropriate matrix and inhibiting their aberrant growth (35). Previous studies have illustrated that the occurrence of anoikis relied on extrinsic pathway and intrinsic pathway (36). Anoikis plays a significant role in tumor metastasis and is closely correlated with tumor development and therapy failure (37). Malignance cells deprive from primary tissue and adapt to abnormal growth elsewhere, contributing to tumor migration. Two main strategies have been demonstrated to achieve anoikis resistance in tumor, including the regulation of the cell adhesion molecules expression and employment of oxidative stress (38). Nevertheless, the accurate mechanisms of anoikis resistance in ccRCC are still need for further study. Past evidence has indicated that anoikis-resistant ccRCC cells displayed insensitiveness to detachment-induced apoptosis and uncontrolled proliferation. Meanwhile, the expression of Tyrosine receptor kinase B (TrkB) in them was higher than parental ccRCC cells (39). Quinazoline-based drugs were described to induce anoikis in RCC through activating focal adhesion survival signaling pathway, which could be a novel therapy method of RCC (40). Moreover, an extracellular matrix deprivation system (EDS) was developed to reverse anoikis resistance of RCC cells *via* downregulating FAK phosphorylation (15).

In this study, we constructed and verified the APM containing seven ARGs, namely BNIP3, CCND1, CEBPB, ERBB2, PECAM1, TIMP1, and UBE2C. An increasing number of studies have demonstrated that these genes were strongly correlated with occurrence and pathogenesis of cancer. As a mitophagy receptor, upregulation of BNIP3 was associated with poorer melanoma patient's endpoint, and BNIP3 knockout in melanoma cells inhibited tumor growth *in vivo* (41). CCND1, a positive cell cycle regulator, was frequently deregulated in tumor and was an indicator

of cancer phenotype and disease development (42). CEBPB was found to be involved in aerobic glycolysis and promote growth of breast cancer (43). On the other hand, overexpression of MIR503 host gene regulated invasion and proliferation of cervical cancer cells and accelerated cell apoptosis by miR-191/CEBPB axis (44). ERBB2 was replicated through elevated gene transcription in various of cancer cells, and tumor growth depended on ERBB2 amplification heavily (45). A series of studies identified that PECAM1 was linked to development of several malignances and had the potential to be a diagnostic and prognostic biomarker in gastric cancer patients (46, 47). The knockdown of TIMP1 expression inhibited metastasis, and proliferation but prompted apoptosis of colon cancer through activating FAK-PI3K/AKT and MAPK pathway (48). And TIMP1 could be an independent prognostic biomarker of OS and disease-free survival for colon cancer patients. As for UBE2C, suppression of UBE2C expression restrained E2-promoted invasion, migration and epithelial mesenchymal transition *in vitro* and *in vivo*, and UBE2C elevation was significantly correlated with higher histologic grade, recurrence, and worse OS in endometrial cancer (49).

The Infiltration of Treg cells was often correlated with worse prognosis in diverse tumors, and decreased Treg cells was found to evoke and promote anti-tumor immune response (50). In our study, the expression levels of BNIP3, CCND1, ERBB2, and PECAM1 were significantly negatively correlated with infiltration level of Treg cells, and CEBPB, TIMP1, and UBE2C were positively associated with infiltration level of Treg cells, suggesting that these genes might affect ccRCC patients' prognosis through regulating infiltration of Treg cells. To explore the potential mechanisms or functions of the ARGs, functional enrichment analysis was conducted. KEGG analysis demonstrated that the seven ARGs were mainly enriched in several types of malignances, including bladder cancer, endometrial cancer, non-small cell lung cancer, pancreatic cancer, and prostate cancer, indicating the intimate relationship between ARGs and different types of tumors.

In summary, we systematically constructed and assessed the APM of ccRCC based on 7 ARGs, and this model could well predict the OS of ccRCC patients. Moreover, we found that these 7 ARGs were closely correlated with immune cell infiltration and immune checkpoint genes. Our study could provide insights for further exploring the role of ARGs in ccRCC and contribute to the progression of personalized and precise therapy strategies.

## Data availability statement

The datasets presented in this study can be found in online repositories. The names of the repository/repositories and accession number(s) can be found in the article/Supplementary Material.

## Author contributions

CS and HS designed the overall study. JZ, ZZ, and ZX revised the paper. YL and ZS drafted the manuscript and performed the data analysis. YB, MF and YD participated in the data

collection. All authors contributed to the article and approved the submitted version.

## Funding

## Conflict of interest

The authors declare that the research was conducted in the absence of any commercial or financial relationships that could be construed as a potential conflict of interest.

The reviewer YZ declared a shared parent affiliation with the authors to the handling editor at the time of review.

## Publisher's note

All claims expressed in this article are solely those of the authors and do not necessarily represent those of their affiliated organizations, or those of the publisher, the editors and the reviewers. Any product that may be evaluated in this article, or claim that may be made by its manufacturer, is not guaranteed or endorsed by the publisher.

## Supplementary material

The Supplementary Material for this article can be found online at: https://www.frontiersin.org/articles/10.3389/fimmu.2023.1171883/full#supplementary-material

## References

1. Sung H, Ferlay J, Siegel RL, Laversanne M, Soerjomataram I, Jemal A, et al. Global cancer statistics 2020: Globocan estimates of incidence and mortality worldwide for 36 cancers in 185 countries. *CA Cancer J Clin* (2021) 71(3):209–49. doi: 10.3322/caac.21660

2. Siegel RL, Miller KD, Fuchs HE, Jemal A. Cancer statistics, 2021. *CA Cancer J Clin* (2021) 71(1):7–33. doi: 10.3322/caac.21654

3. Gulati S, Vaishampayan U. Current state of systemic therapies for advanced renal cell carcinoma. *Curr Oncol Rep* (2020) 22(3):26. doi: 10.1007/s11912-020-0892-1

4. Fisher R, Gore M, Larkin J. Current and future systemic treatments for renal cell carcinoma. *Semin Cancer Biol* (2013) 23(1):38–45. doi: 10.1016/j.semcancer.2012.06.004

5. Turajlic S, Xu H, Litchfield K, Rowan A, Chambers T, Lopez JI, et al. Tracking cancer evolution reveals constrained routes to metastases: Tracerx renal. *Cell* (2018) 173(3):581–94. doi: 10.1016/j.cell.2018.03.057

6. Bagcchi S. Sunitinib still Fi rst-line therapy for metastatic renal cancer. *Lancet Oncol* (2014) 15(10):e420. doi: 10.1016/S1470-2045(14)70366-3

7. Tatsugami K, Oya M, Kabu K, Akaza H. Evaluation of efficacy and safety of sorafenib in kidney cancer patients aged 75 years and older: A propensity score-matched analysis. *Br J Cancer* (2018) 119(2):241–7. doi: 10.1038/s41416-018-0129-3

8. Randrup Hansen C, Grimm D, Bauer J, Wehland M, Magnusson NE. Effects and side effects of using sorafenib and sunitinib in the treatment of metastatic renal cell carcinoma. *Int J Mol Sci* (2017) 18(2):461. doi: 10.3390/ijms18020461

9. Janiszewska M, Primi MC, Izard T. Cell adhesion in cancer: Beyond the migration of single cells. *J Biol Chem* (2020) 295(8):2495–505. doi: 10.1074/jbc.REV119.007759

10. Han H-J, Sung JY, Kim S-H, Yun U-J, Kim H, Jang E-J, et al. Fibronectin regulates anoikis resistance *Via* cell aggregate formation. *Cancer Lett* (2021) 508:59–72. doi: 10.1016/j.canlet.2021.03.011

11. Zhong X, Rescorla FJ. Cell surface adhesion molecules and adhesion-initiated signaling: Understanding of anoikis resistance mechanisms and therapeutic opportunities. *Cell Signal* (2012) 24(2):393–401. doi: 10.1016/j.cellsig.2011.10.005

12. Haun F, Neumann S, Peintner L, Wieland K, Habicht J, Schwan C, et al. Identification of a novel anoikis signalling pathway using the fungal virulence factor gliotoxin. *Nat Commun* (2018) 9(1):3524. doi: 10.1038/s41467-018-05850-w

13. She K, Yang W, Li M, Xiong W, Zhou M. Faim2 promotes non-small cell lung cancer cell growth and bone metastasis by activating the Wnt/?-catenin pathway. *Front In Oncol* (2021) 11:690142. doi: 10.3389/fonc.2021.690142

14. Takagi Y, Sakai N, Yoshitomi H, Furukawa K, Takayashiki T, Kuboki S, et al. High expression of krüppel-like factor 5 is associated with poor prognosis in patients with colorectal cancer. *Cancer Sci* (2020) 111(6):2078–92. doi: 10.1111/cas.14411

15. Wang L, Li C, Wang J, Yang G, Lv Y, Fu B, et al. Transformable ecm deprivation system effectively suppresses renal cell carcinoma by reversing anoikis resistance and increasing chemotherapy sensitivity. *Adv Mater* (2022) 34(43):e2203518. doi: 10.1002/adma.202203518

16. Takaha N, Sowa Y, Takeuchi I, Hongo F, Kawauchi A, Miki T. Expression and role of Hmga1 in renal cell carcinoma. *J Urol* (2012) 187(6):2215–22. doi: 10.1016/j.juro.2012.01.069

17. Rebhan M, Chalifa-Caspi V, Prilusky J, Lancet D. Genecards: Integrating information about genes, proteins and diseases. *Trends Genet* (1997) 13(4):163. doi: 10.1016/s0168-9525(97)01103-7

18. Rouillard AD, Gundersen GW, Fernandez NF, Wang Z, Monteiro CD, McDermott MG, et al. The harmonizome: A collection of processed datasets gathered to serve and mine knowledge about genes and proteins. *Database (Oxford)* (2016) 2016:1–16. doi: 10.1093/database/baw100

19. Robinson MD, McCarthy DJ, Smyth GK. Edger: A bioconductor package for differential expression analysis of digital gene expression data. *Bioinformatics* (2010) 26 (1):139–40. doi: 10.1093/bioinformatics/btp616

20. Liu J, Lichtenberg T, Hoadley KA, Poisson LM, Lazar AJ, Cherniack AD, et al. An integrated tcga pan-cancer clinical data resource to drive high-quality survival outcome analytics. *Cell* (2018) 173(2):400–16. doi: 10.1016/j.cell.2018.02.052

21. Simon N, Friedman J, Hastie T, Tibshirani R. Regularization paths for cox's proportional hazards model *Via* coordinate descent. *J Stat Softw* (2011) 39(5):1–13. doi: 10.18637/jss.v039.i05

22. Tibshirani R. The lasso method for variable selection in the cox model. *Stat Med* (1997) 16(4):385–95. doi: 10.1002/(sici)1097-0258(19970228)16:4<385::aid-sim380>3.0.co;2-3

23. Goldman MJ, Craft B, Hastie M, Repečka K, McDade F, Kamath A, et al. Visualizing and interpreting cancer genomics data *Via* the xena platform. *Nat Biotechnol* (2020) 38(6):675–8. doi: 10.1038/s41587-020-0546-8

24. Chen F, Chandrashekar DS, Varambally S, Creighton CJ. Pan-cancer molecular subtypes revealed by mass-Spectrometry-Based proteomic characterization of more than 500 human cancers. *Nat Commun* (2019) 10(1):5679. doi: 10.1038/s41467-019-13528-0

25. Thorsson V, Gibbs DL, Brown SD, Wolf D, Bortone DS, Ou Yang T-H, et al. The immune landscape of cancer. *Immunity* (2018) 48(4):812–30. doi: 10.1016/j.immuni.2018.03.023

26. Wu T, Dai Y. Tumor microenvironment and therapeutic response. *Cancer Lett* (2017) 387:61–8. doi: 10.1016/j.canlet.2016.01.043

27. Lei X, Lei Y, Li J-K, Du W-X, Li R-G, Yang J, et al. Immune cells within the tumor microenvironment: Biological functions and roles in cancer immunotherapy. *Cancer Lett* (2020) 470:126–33. doi: 10.1016/j.canlet.2019.11.009

28. Warde-Farley D, Donaldson SL, Comes O, Zuberi K, Badrawi R, Chao P, et al. The genemania prediction server: Biological network integration for gene prioritization and predicting gene function. *Nucleic Acids Res* (2010) 38(Web Server issue):W214–W20. doi: 10.1093/nar/gkq537

29. D'Avella C, Abbosh P, Pal SK, Geynisman DM. Mutations in renal cell carcinoma. *Urol Oncol* (2020) 38(10):763–73. doi: 10.1016/j.urolonc.2018.10.027

30. Hsieh JJ, Purdue MP, Signoretti S, Swanton C, Albiges L, Schmidinger M, et al. Renal cell carcinoma. *Nat Rev Dis Primers* (2017) 3:17009. doi: 10.1038/nrdp.2017.9

31. Zeng X, Zhu C, Zhu X. Dusp4 promotes the carcinogenesis of ccrcc *Via* negative regulation of autophagic death. *Biosci Biotechnol Biochem* (2021) 85(8):1839–45. doi: 10.1093/bbb/zbab111

32. Bergers G, Hanahan D. Modes of resistance to anti-angiogenic therapy. *Nat Rev Cancer* (2008) 8(8):592–603. doi: 10.1038/nrc2442

33. Molina AM, Lin X, Korytowsky B, Matczak E, Lechuga MJ, Wiltshire R, et al. Sunitinib objective response in metastatic renal cell carcinoma: Analysis of 1059 patients treated on clinical trials. *Eur J Cancer* (2014) 50(2):351–8. doi: 10.1016/j.ejca.2013.08.021

34. Motzer RJ, Hutson TE, Tomczak P, Michaelson MD, Bukowski RM, Rixe O, et al. Sunitinib versus interferon Alfa in metastatic renal-cell carcinoma. *N Engl J Med* (2007) 356(2):115–24. doi: 10.1056/NEJMoa065044

35. Kakavandi E, Shahbahrami R, Goudarzi H, Eslami G, Faghihloo E. Anoikis resistance and oncoviruses. *J Cell Biochem* (2018) 119(3):2484–91. doi: 10.1002/jcb.26363

36. Sun Z, Zhao Y, Wei Y, Ding X, Tan C, Wang C. Identification and validation of an anoikis-associated gene signature to predict clinical character, stemness, idh mutation, and immune filtration in glioblastoma. *Front Immunol* (2022) 13:939523. doi: 10.3389/fimmu.2022.939523

37. Wang J, Luo Z, Lin L, Sui X, Yu L, Xu C, et al. Anoikis-associated lung cancer metastasis: Mechanisms and therapies. *Cancers (Basel)* (2022) 14(19):4791. doi: 10.3390/cancers14194791

38. Taddei ML, Giannoni E, Fiaschi T, Chiarugi P. Anoikis: An emerging hallmark in health and diseases. *J Pathol* (2012) 226(2):380–93. doi: 10.1002/path.3000

39. Zhang P, Xing Z, Li X, Song Y, Zhao J, Xiao Y, et al. Tyrosine receptor kinase b silencing inhibits Anoikis–Resistance and improves anticancer efficiency of sorafenib in human renal cancer cells. *Int J Oncol* (2016) 48(4):1417–25. doi: 10.3892/ijo.2016.3356

40. Sakamoto S, Schwarze S, Kyprianou N. Anoikis disruption of focal adhesion-akt signaling impairs renal cell carcinoma. *Eur Urol* (2011) 59(5):734–44. doi: 10.1016/j.eururo.2010.12.038

41. Vara-Pérez M, Rossi M, Van den Haute C, Maes H, Sassano ML, Venkataramani V, et al. Bnip3 promotes hif-1α-Driven melanoma growth by curbing intracellular iron homeostasis. *EMBO J* (2021) 40(10):e106214. doi: 10.15252/embj.2020106214

42. Musgrove EA, Caldon CE, Barraclough J, Stone A, Sutherland RL. Cyclin d as a therapeutic target in cancer. *Nat Rev Cancer* (2011) 11(8):558–72. doi: 10.1038/nrc3090

43. Li W, Tanikawa T, Kryczek I, Xia H, Li G, Wu K, et al. Aerobic glycolysis controls myeloid-derived suppressor cells and tumor immunity *Via* a specific cebpb isoform in triple-negative breast cancer. *Cell Metab* (2018) 28(1):87–103. doi: 10.1016/j.cmet.2018.04.022

44. Hu YL, Zhang YX, Liu N, Liu H, Yuan YC. Lncrna Mir503hg regulated cell viability, metastasis and apoptosis of cervical cancer *Via* mir-191/Cebpb axis. *Eur Rev Med Pharmacol Sci* (2021) 25(8):3200–10. doi: 10.26355/eurrev_202104_25728

45. Vermeulen Z, Segers VFM, De Keulenaer GW. Erbb2 signaling at the crossing between heart failure and cancer. *Basic Res Cardiol* (2016) 111(6):60. doi: 10.1007/s00395-016-0576-z

46. Li Y, Guo XB, Wei YH, Kang XL. Serum Cxcl13 and pecam-1 can be used as diagnostic and prognostic markers in elderly patients with gastric cancer. *Clin Transl Oncol* (2021) 23(1):130–8. doi: 10.1007/s12094-020-02403-w

47. Yang J-F, Shi S-N, Xu W-H, Qiu Y-H, Zheng J-Z, Yu K, et al. Screening, identification and validation of Ccnd1 and Pecam1/Cd31 for predicting prognosis in renal cell carcinoma patients. *Aging (Albany NY)* (2019) 11(24):12057–79. doi: 10.18632/aging.102540

48. Song G, Xu S, Zhang H, Wang Y, Xiao C, Jiang T, et al. Timp1 is a prognostic marker for the progression and metastasis of colon cancer through fak-Pi3k/Akt and mapk pathway. *J Exp Clin Cancer Res* (2016) 35(1):148. doi: 10.1186/s13046-016-0427-7

49. Liu Y, Zhao R, Chi S, Zhang W, Xiao C, Zhou X, et al. Is upregulated by estrogen and promotes epithelial-mesenchymal transition *Via* P53 in endometrial cancer. *Mol Cancer Res* (2020) 18(2):204–15. doi: 10.1158/1541-7786.MCR-19-0561

50. Tanaka A, Sakaguchi S. Regulatory T cells in cancer immunotherapy. *Cell Res* (2017) 27(1):109–18. doi: 10.1038/cr.2016.151

# Glossary

| Abbreviation | Full name |
| --- | --- |
| APM | Anoikis prognostic model |
| ARGs | Anoikis-related genes |
| ATCC | American Type Cultural Collection |
| AUC | Area under curve |
| BNIP3 | Bcl-2/adenovirus E1B 19kDa interacting protein 3 |
| CCND1 | Cyclin D1 |
| ccRCC | Clear cell renal cell carcinoma |
| CEBPB | CCAAT/enhancer-binding protein beta |
| CPTAC | Clinical Proteomic Tumor Analysis Consortium |
| EARS2 | Glutamyl-tRNA synthetase 2 |
| EDS | Extracellular matrix deprivation system |
| ERBB2 | Epidermal growth factor receptor 2 |
| FAIM2 | Fas apoptotic inhibitory molecule 2 |
| FBS | Fetal bovine serum |
| GO | Gene Ontology |
| GTEx | Genotype-Tissue Expression |
| IHC | Immunohistochemistry |
| KEGG | Kyoto Encyclopedia of Genes and Genomes |
| KLF5 | Kruppel-like factor 5 |
| K-M | Kaplan-Meier |
| LASSO | Least absolute shrinkage and selection operator |
| OS | Overall survival |
| PECAM1 | Platelet endothelial cell adhesion molecule-1 |
| RCC | Renal cell carcinoma |
| ROC | Receiver operating characteristic |
| TCGA | The Cancer Genome Atlas |
| TIMP1 | Tissue inhibitor of metalloprotease 1 |
| TME | Tumor microenvironment |
| TPGs | Tumor prognostic genes |
| TrKB | Tyrosine receptor kinase B |
| UBE2C | Ubiquitin-conjugating enzyme E2C |